Electronic Supplementary Information

Accurate engineering of hexagonal hollow carbon nitride with carbon vacancies: Enhanced photocatalytic H_2 evolution and its mechanism

Xueru Chen, [a] Xin Li, [a] Xue Li, [a] Huimin Lu, [a] Lei Wang, [a] Qianqian Liu, [c] Hongping Li, [b] Jing Ding, *[a] Hui Wan [a] and Guofeng Guan *[a]

[a] *State Key Laboratory of Materials-Oriented Chemical Engineering, College of Chemical Engineering, Jiangsu National Synergetic Innovation Center for Advanced Materials, Nanjing Tech University, Nanjing 210009, P.R. China;*

[b] *Institute for Energy Research of Jiangsu University, Jiangsu University, Zhenjiang 212013, P.R. China;*

[c] *Research Center for Nanophotonic and Nanoelectronic Materials, School of Materials Science and Engineering, Suzhou University of Science and Technology, Suzhou 215009, P.R. China;*

Materials: Melamine (MA, 99%), cyanuric acid (CA, 98%) and triethanolamine (TEOA, AR) were all purchased from Aladdin Industrial Inc. Pluronic P123 (average Mn ~ 5800) was bought from Sigma-Aldrich. Sulfuric acid (H_2SO_4, 98%) was obtained from Shanghai Lingfeng Chemical Co., Ltd. All the chemicals were used as received.

Characterization: X-ray diffraction (XRD) measurements were collected from Smartlab diffractometer (RIGAKU, Japan) from 10° to 80° with a step increment of 10°/min at 100 mA and 40kV. Fourier transform infrared (FT-IR) spectroscopy in the wavelength ranging from 4000-400 cm^{-1} was acquired from Thermo Nicolet 6700 spectrometer (United States) employing the anhydrous KBr as dispersing agent. The scanning electron microscope (SEM, Hitachi S4800) and transmission electron microscopy (TEM, JEOL JEM-2100) were used to observe the morphology. Nitrogen adsorption-desorption measurements were conducted at -196 °C on Micromeritics ASAP 2020 to determine the surface area by Brunauer-Emmett-Tell (BET) method and pore size distribution by Barret-Joyner-Halenda (BJH) method. The X-ray photoelectron spectroscopy (XPS) was operated on PHI-5000 Versa Probe system (Britain) and the C 1s binding energy centred at 284.6 eV. Ultraviolet visible (UV-vis) diffuse reflectance spectroscopy was examined by Shimadzu UV-3600 spectrophotometer equipped with $BaSO_4$ tablet as the absorb standard. The investigation of photoluminescence (PL) properties was performed on Hitachi F-4500 at an excitation wavelength of 370 nm. Elemental analysis was carried on Elementar Vario EL (Germany) to survey the content of C, N, H and S elements.

Photocatalytic H_2 evolution experiment: The photocatalytic performance was evaluated by photocatalytic hydrogen evolution from water splitting in a top-irradiation vessel under visible light irradiation. A 300 W Xe-lamp (CEL-HXF300, AuLight, China) equipped with 400 nm cutoff filter was installed above the photo-reactor. Generally, the experiments were carried out in the suspension solution consisting of 50 mg catalyst and 10 vol % triethanolamine (TEOA) which acted as hole scavenger. Pt (3 wt %) was loaded on the surface of the photocatalyst as cocatalyst by in situ photodeposition of H_2PtCl_6. The system was evacuated and replenished with N_2 for several times to remove air. Subsequently, the test was proceeded for 4 h under visible light irradiation with continuous stirring to ensure its homogeneity. The evolved H_2 was quantified for each hour by gas chromatography system (GC 7860 Plus) outfitting a thermal conductivity detector. The apparent quantum efficiency (AQE) for H_2 evolution was evaluated by band-pass filters centered at 380, 420, 450, 475, 500 and 550 nm according to the following formula:

$$AQE(\%) = \frac{2 \times \text{Number of evolved } H_2 \text{ molecules}}{\text{Number of incident photons}} \times 100\%$$

Photoelectrochemical measurements: The photoelectrochemical characterizations were conducted in 0.5 M Na_2SO_4 solution with the electrochemical workstation (Chenhua, CHI 660E, China) equipped with a standard three-electrode system, which included a counter electrode (Pt plate), a reference electrode (Ag/AgCl) and a work electrode. In the preparation of work electrode, 2 mg sample, 0.4 ml ethanol and 40 μL Nafion were well dispersed by sonication and coated on a conductive FTO glass (1 cm × 3 cm). Then the working electrode was fabricated after drying overnight. During

the measurement, a 300 W Xenon lamp equipped with 400 nm-cutoff filter was adopted as the light source. The Mott-Schottky plot was conducted in the same system with frequency of 2000, 3000 and 4000 Hz.

Density-Functional Theory (DFT) calculation: Electrostatic Potential maps (ESP, isosurfaces = 0.001 e/Bohr^3) and Noncovalent Interactions (NCI) [2] were calculated on Gaussian 09 D 0.1[1], analyzed by Multiwfn 3.8 [3] and displayed by VMD 1.9.3 (molecular visualization) [4]. Moreover, NCI was analyzed by reduced density gradient (RDG).

Reference

[1] R.A. Gaussian 09, M.J. Frisch, G.W. Trucks, H.B. Schlegel, G.E. Scuseria, M. A. Robb, J.R. Cheeseman, G. Scalmani, V. Barone, G.A. Petersson, H. Nakatsuji, X. Li, M. Caricato, A. Marenich, J. Bloino, B.G. Janesko, R. Gomperts, B. Mennucci, H.P. Hratchian, J.V. Ortiz, A.F. Izmaylov, J.L. Sonnenberg, D. Williams-Young, F. Ding, F. Lipparini, F. Egidi, J. Goings, B. Peng, A. Petrone, T. Henderson, D. Ranasinghe, V.G. Zakrzewski, J. Gao, N. Rega, G. Zheng, W. Liang, M. Hada, M. Ehara, K. Toyota, R. Fukuda, J. Hasegawa, M. Ishida, T. Nakajima, Y. Honda, O. Kitao, H. Nakai, T. Vreven, K. Throssell, J.A. Montgomery Jr., J.E. Peralta, F. Ogliaro, M. Bearpark, J.J. Heyd, E. Brothers, K.N. Kudin, V.N. Staroverov, T. Keith, R. Kobayashi, J. Normand, K. Raghavachari, A. Rendell, J.C. Burant, S. S. Iyengar, J. Tomasi, M. Cossi, J.M. Millam, M. Klene, C. Adamo, R. Cammi, J. W. Ochterski, R.L. Martin, K. Morokuma, O. Farkas, J.B. Foresman and D.J. Fox, *Gaussian, Inc.*,

Wallingford CT, 2016.

[2] E.R. Johnson, S. Keinan, P. Mori-Sa´nchez, J. Contreras-Garcı´a, A.J. Cohen and W. Yang, *J. Am. Chem. Soc.,* 2010, **132**, 6498-6506.

[3] T. Lu, F.W and Chen, , *J. Comput. Chem.,* 2012, **33**, 580-592.

[4] W. Humphrey, A. Dalke and K. Schulten, *J. of Molec. Graphics,* 1996, **14**, 33-38.

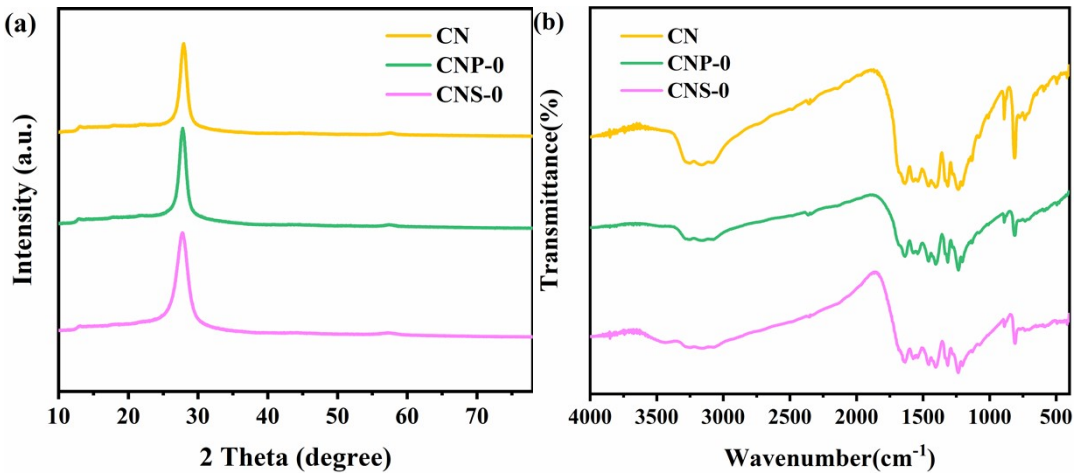

Fig. S1 XRD and FT-IR spectra of CN, CNP-0 and CNS-0.

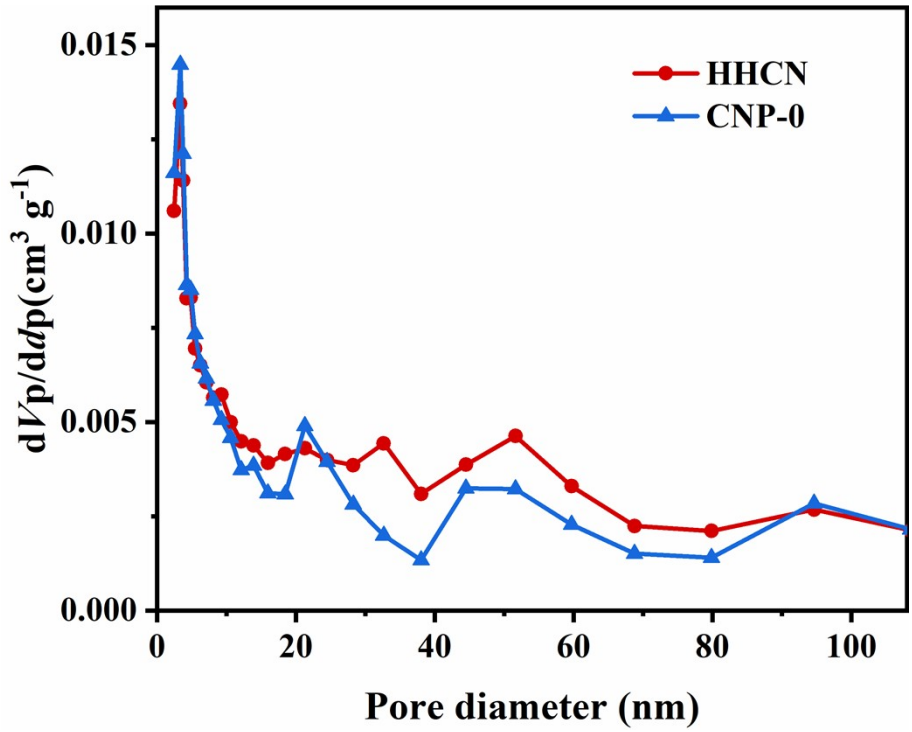

Fig. S2 Pore size distribution of HHCN and CNP-0.

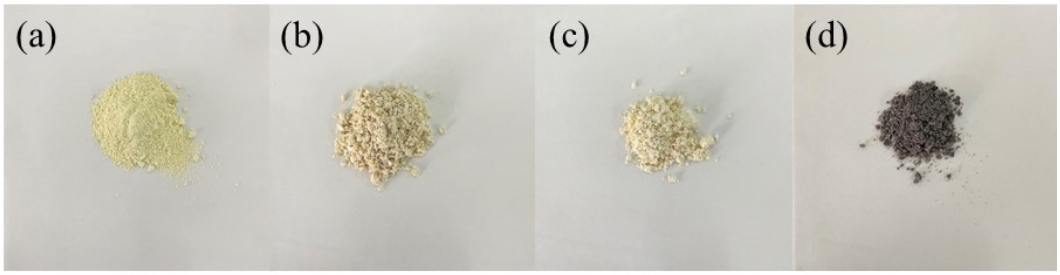

Fig. S3 Photograph of (a) g-C_3N_4, (b) HHCN, (c) CNP-0 and (d) CNS-0.

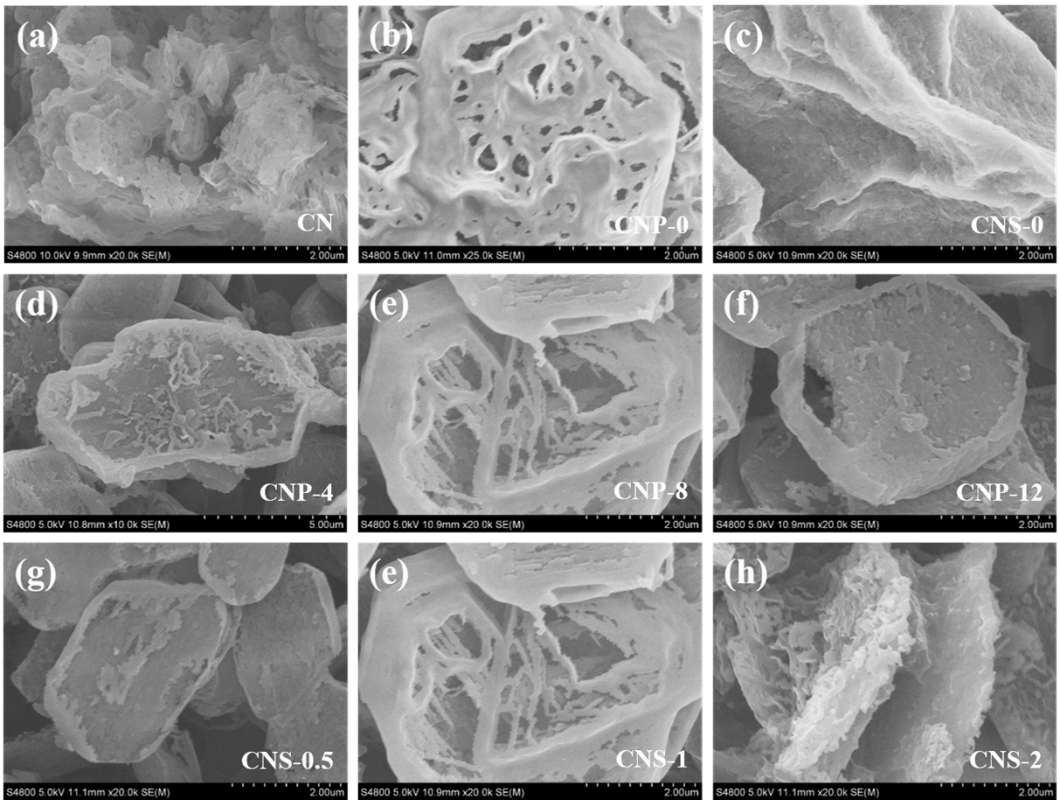

Fig. S4 SEM of (a) CN, (b) CNP-0, (c) CNS-0; SEM of samples with different P123 dosage: (d) CNP-4, (e) CNP-8 (HHCN) and (f) CNP-12; SEM of samples with different H_2SO_4 concentration: (g) CNS-0.5, (e) CNS-1 (HHCN) and (h) CNS-2.

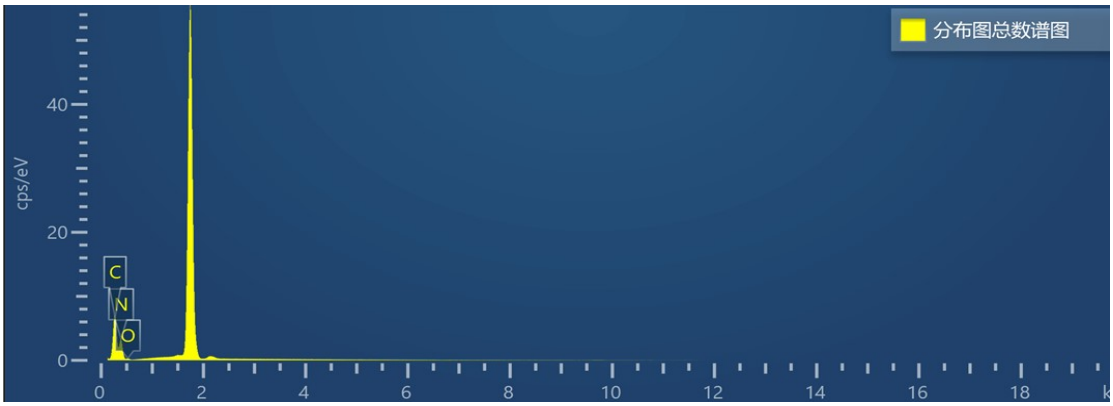

Fig. S5 EDX of HHCN.

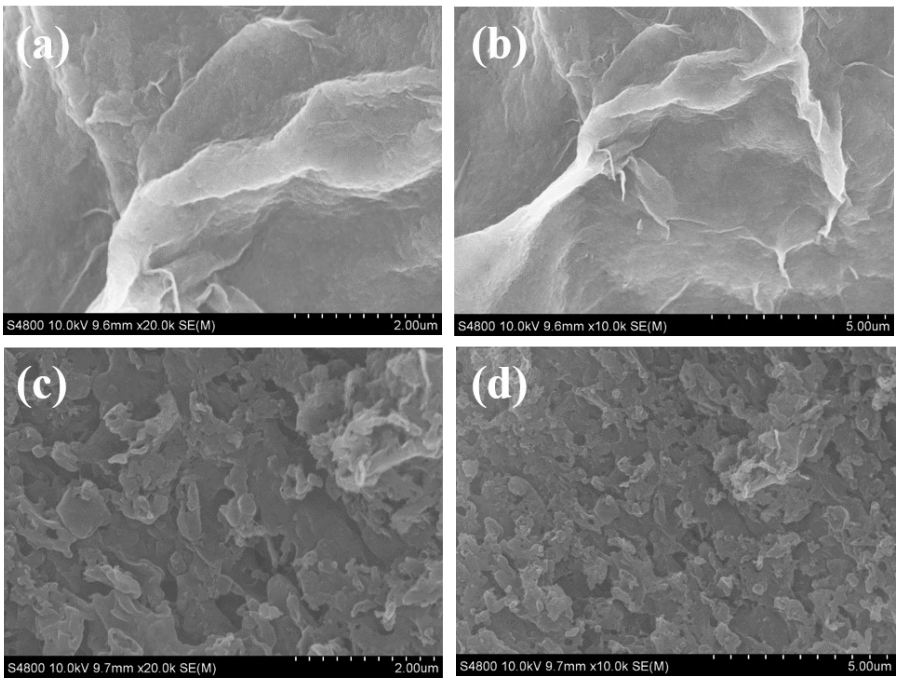

Fig. S6 SEM of CNC (a-b) and CNN (c-d).

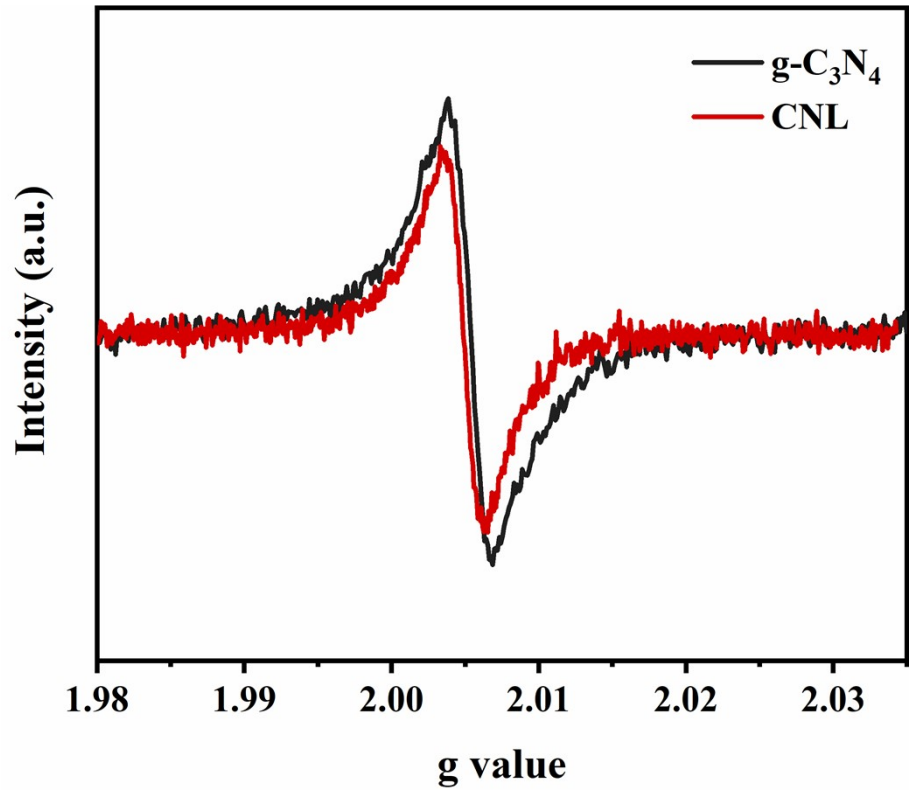

Fig. S7 EPR spectra of CNL and g-C_3N_4.

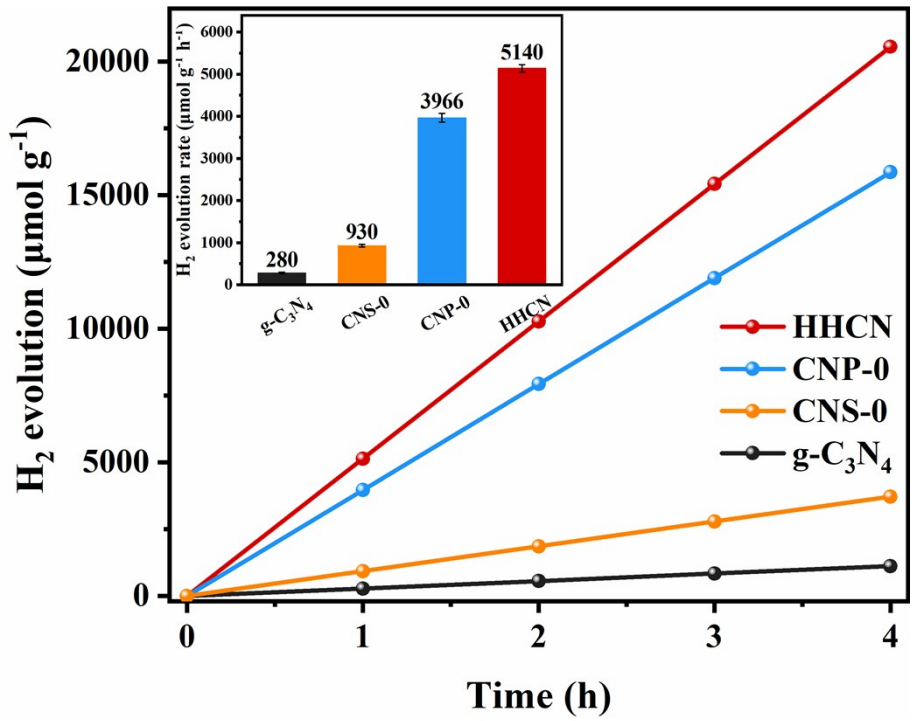

Fig. S8 The photocatalytic H_2 evolution performance of HHCN, CNP-0, CNS-0 and g-C_3N_4 (inset: The corresponding H_2 evolution rate).

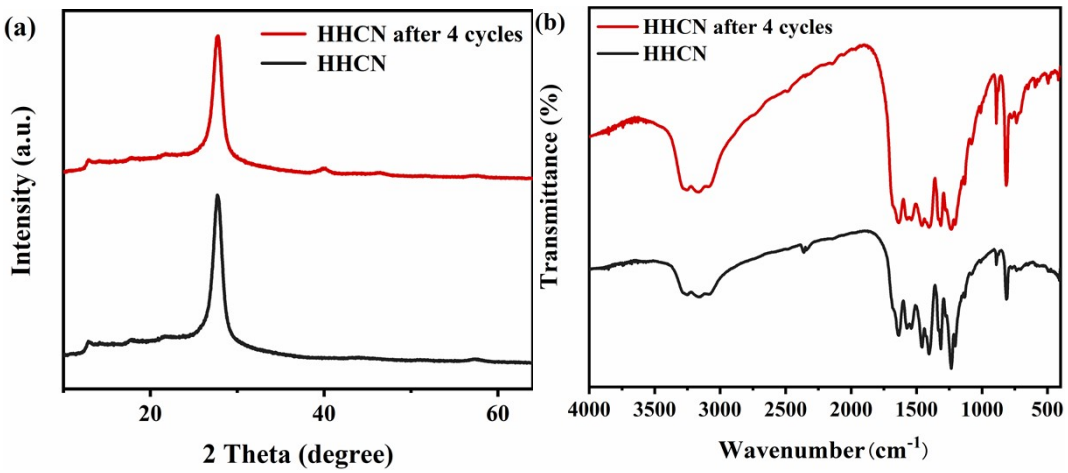

Fig. S9 XRD (a) and FT-IR (b) of HHCN after 4 cycles.

Table S1 Specific surface area, pore volume and pore size of HHCN and g-C_3N_4.

Sample	S_{BET} [m^2 g^{-1}]	Total pore volume [cm^3 g^{-1}]	Average pore diameter [nm]
HHCN	114	0.45	15.7
CNP-0	109	0.4	14.5
CN	81	0.3	14.9
g-C_3N_4	10	0.03	11.9

Table S2 Element contents and C/N atomic ratio of HHCN and g-C_3N_4.

Sample	C [wt%]	N [wt%]	H [wt%]	S [wt%]	C/N atomic ratio	C/H atomic ratio
HHCN	34.59	62.25	1.939	0	0.648	1.487
g-C_3N_4	35.21	62.57	2.215	0	0.657	1.325